Development and performance analysis of a novel multi-zone hybrid desiccant cooling system

Shuo Liu [a], Chang-Ho Jeong [b], Myoung-Souk Yeo *[c].

[a] Department of Architecture and Architectural Engineering, Graduate School, Seoul National University, Seoul, Korea, 2019-34430@snu.ac.kr

[b] Division of Architecture for Urban Planning & Real Estate Development, The University of Suwon, Hwaseong, Korea, chjeong@suwon.ac.kr

[c] Institute of Construction and Environmental Engineering, Department of Architecture and Architectural Engineering, Seoul National University, Seoul, Korea, msyeo@snu.ac.kr

Abstract. This study proposed a novel multi-zone applicable hybrid desiccant cooling system (MHDC) that uses condensing heat from the condenser to regenerate the solid desiccant and applied it as an outdoor air unit (OAU) with demand-controlled ventilation (DCV) in order to control the indoor humidity and air quality (IAQ). Indoor temperature and humidity control effect and system energy use were analysed compared to a conventional packaged terminal air-conditioning (PTAC) system with the heat recovery wheel (HRW) assisted OAU. The simulation result shows that in a typical high-rise building with high air tightness, The CO_2 concentration in bedrooms can reach up to 3686 ppm when PTACs operate without fresh air. Without the dehumidification process, the introduction of fresh air will increase the relative humidity most of the occupancy time. The MHDC system adopted DCV can maintain IAQ except for a short period of cooking time and can handle the fresh air latent load while controlling indoor humidity without a separate regeneration heat source. However, due to the air volume limitation of OAU, the instantaneous dehumidification capacity of the MHDC system is not sufficient, resulting in a short time required to process the indoor humidity to 50 % level when the system initially started. Although the operation of the MHDC system increases the energy use of the OAU, the decrease in the latent load of zone level PTACs makes the total energy use is almost equal to the PTAC system with HRW assisted OAU, 606 kWh and 605 kWh respectively, while obtaining better indoor thermal comfort and IAQ. This study can prove that the proposed MHDC system is a possible alternative system to a conventional multi-zone air-conditioning system that can provide energy savings and thermal comfort.

Keywords. Multi-zone air conditioning system, demand-controlled ventilation, outdoor air unit, Indoor air quality, Dehumidification, energy use.
DOI: https://doi.org/10.34641/clima.2022.188

1. Introduction

Indoor environment control is one of the most significant indicators to evaluate the performance of an air conditioning system. Indoor humidity control should be considered while performing an effective indoor temperature control. It is demonstrated that the growth of human health-related bacteria and melds can be effectively inhibited under 40 ~ 60 % relative humidity conditions [1]. The mismatch between the indoor sensible heat ratio (SHR) and sensible heat ratio of general air conditioning unit leads to the problem associated with indoor humidity control [2]. In addition, the proportion of latent load to total indoor load is increasing due to the requirement of fresh outdoor air and changing lifestyle of occupants [3]. Therefore, discomfort caused by humidity has gradually become the main problem of indoor comfort control because general domestic air-conditioning units do not possess an effective dehumidification capacity. Currently, condensation dehumidification systems are widely used in practical applications due to their compact system structure and convenience maintenance. Generally, direct expansion (DX) cooling coils or chilled water-cooling coils are used to reduce the air temperature below the dew point temperature. The cooling coil operates in a wet coil state, which causes the growth of fungi and affects indoor air quality and personnel health [4]. And the sub-

cooling and re-heating process in the condensation dehumidification system causes unnecessary energy use [5]. Focusing on the possibility of miniaturization and dehumidification capacity, this study assesses the solid desiccant dehumidification system which mainly absorbs the moisture through the solid desiccant composed desiccant wheels. Existing studies have discussed the thermal comfort and energy-saving effects of various solid desiccant dehumidification systems and combined desiccant wheels with various cooling equipment to become a hybrid solid desiccant cooling system (HDC). In addition to responding the indoor load, the cooling equipment has to handle the adsorption heat generated by the dehumidification process. Mainstream cooling equipment includes DX cooling coil, direct evaporative cooler (DEC), in-direct evaporative cooler (IEC), and regenerative evaporative cooler (REC). These HDC systems can effectively control temperature and humidity; however, a separate heating coil provides the heat required for desiccant regeneration, which reduces the system's energy efficiency and structural advantages [6-9]. The energy use of the regeneration electric heater accounts for more than 45% of the system's total energy use [10]. The regeneration temperature of most desiccants is mainly in the range of 60 ^{o}C and 90 ^{o}C. Even if desiccants exist with regeneration temperatures lower than 50 ^{o}C, they cannot be regenerated by outdoor high-temperature air [11]. Therefore, in addition to the development of low-temperature regeneration desiccant [12] the use of renewable energy and low-grade waste heat become a significant research direction to solve the regeneration heat consumption. Ali et al. [13, 14] proposed a decoupling cooling system that combined the solar energy regenerated solid desiccant system with a radiant cooling system and optimized the design parameters of the solar collectors. Additionally, they experimentally investigated indoor thermal comfort during winter. However, solar collectors may not produce adequate regeneration heat output under high outdoor humidity and low solar radiation [15]. Therefore, focusing on the trade-off between the simple system structure and stable regeneration heat output, this paper assessed the heat-pump assisted hybrid solid desiccant cooling system (HPDC) that regenerated the desiccant wheel through the condenser's condensation heat. Some extant studies have focused on HPDC systems with the evaporator located downstream of the desiccant wheel (HPDC-D). Sheng et al. [16] studied the effect of outdoor conditions on the regeneration temperature and proposed that the COP of the heat pump increases with increasing outdoor temperature. Jia et al. [17] analysed the effect of different inlet air conditions and regeneration temperature on the sensible heat ratio of a heat pump in the HPDC-D system. Nie et al. [18, 19] observed that the increase in outdoor humidity caused increased heat pump energy use and a decrease in COP. Ge et al. [20] analysed the HPDC-D system and condensing dehumidification system regarding their exergy efficiency and clarified the relationship between regeneration air humidity and regeneration temperature. The HPDC system with the evaporator located upstream of the desiccant wheel (HPDC-U) is proposed to improve the dehumidification performance and reduce the dehumidification load by pre-cooling and pre-dehumidification. Belguith et al. [21] observed the negative effect of humidity on dehumidification performance and suggested the issue of ineffective supply air temperature control. In a previous study [22], the performances of HPDC-U, HPDC-D, and condensation dehumidification systems were compared regarding their energy use and energy efficiency.

Current research on dehumidification systems mainly focuses on the performance of systems with different system structures and the temperature and humidity control effect for a single space or experimental space. For air conditioning systems serving multi zone, how to effectively control the humidity of each space while ensuring indoor air quality (IAQ) is a research issue that needs more attention. To ensure the IAQ in each space, separated outdoor air units are usually installed, and the minimum outdoor air volume is usually determined by the building type and the number of people in the room. Demand controlled ventilation (DCV) is an effective approach to reduce the outdoor air cooling/heating load compared to constant volume ventilation systems by reducing the outdoor air volume during most of the operation time, which provides a great opportunity to reduce the energy use of fan operation and HVAC system. [23]. Luigi et al. [24] demonstrated a 33 % reduction in total annual primary energy use for air handling units (AHUs) with the DCV compared to conventional constant flow ventilation. In the case study about four school and office buildings, Bart et al. [25] showed that the fan energy use could be reduced by 50 % to 55 % with the DCV due to its variable outdoor air volume. Sun et al. [26] implemented a CO_2 based adaptive DCV in a multi-zone office building in Hong-Kong and also demonstrated that the fan energy use under the DCV strategy is significantly lower compared to the constant air flow system.

In view of the high energy use in outdoor air treatment process and the multi-zone humidity control problem, it is necessary to investigate the feasibility of a multi-zone applicable hybrid desiccant cooling (MHDC) system combined HPDC-U with DCV. The following innovative research is conducted in this paper. As a reference group, indoor humidity control and IAQ problems in the commonly used packaged terminal air conditioning units (PTAC) without outdoor air are demonstrated. The effects of adopting DCV on indoor environment are also discussed. This study verifies the accuracy of the desiccant wheel model based on the analytic solution. The improvement of indoor humidity

environment by combining HPDC-U system with DCV is analyzed and the system energy use is compared to the outdoor air unit (OAU) with heat recovery wheel (HRW).

2. Research methodology

2.1 System configurations and control logics

Case1: conventional PTAC without the outdoor air.

The conventional PTAC mainly consists of a direct expansion cooling coil, which is responsible for regulating the indoor temperature in summer, and an electric auxiliary heater which is designed for heating in winter. PTACs are installed in each room and there is no OAU. The distribution of the PTAC is shown in Fig. 1. (The outdoor unit placed outside is not shown in the figure.) Case 1 is intended to serve as a reference group to illustrate the problems of indoor humidity control and IAQ in conventional household air conditioner.

Case2: conventional PTAC with heat recovery wheel assisted DCV approach OAU.

Compared to conventional PTACs, IAQ in buildings with OAU can be effectively controlled. However, the introduction of outdoor air increases the cooling load of the cooling equipment, therefore, a heat exchanger wheel is used to induce the heat exchange between the outdoor air and the indoor return air as shown in the Fig. 2. The outdoor air after heat exchange is then mixed with the indoor return air and cooled by PTACs. Considering the impact of outdoor air cooling load on the system energy efficiency, the outdoor fresh air volume is controlled by DCV method to reduce the energy use while meeting IAQ.

Case3: conventional PTAC with HPDC-U assisted DCV approach OAU

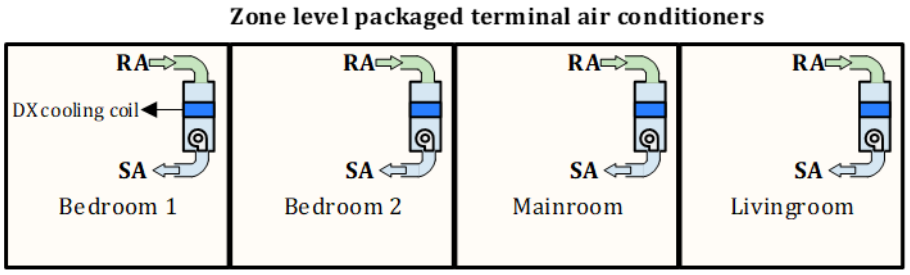

Fig. 1 - The distribution of the PTAC.

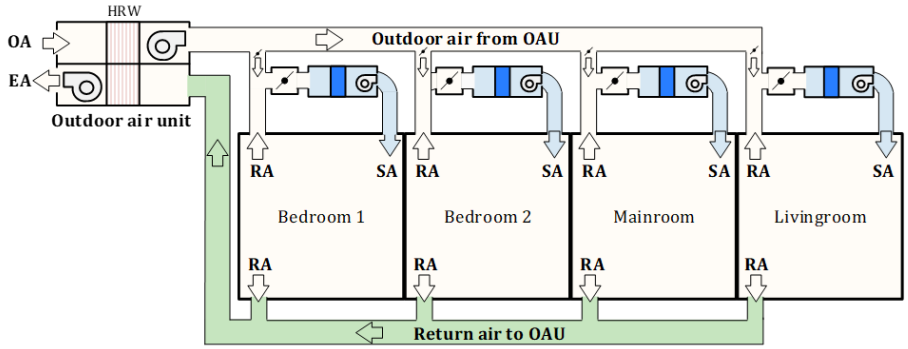

Fig. 2 – Diagram of zone level PTACs and the heat recovery wheel assisted OAU.

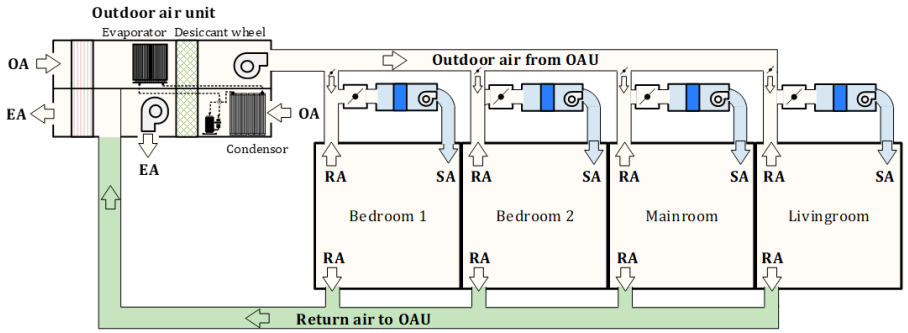

Fig. 3 – Diagram of the HPDC-U assisted OAU.

Although previous studies have demonstrated the ability of HPDC-U systems to effectively control indoor humidity in a single-zone, for HPDC-U systems serving multi-zone with variable latent load profile and total outdoor air volumes, the multi-zone humidity control effect and stability of the regeneration process need to be proven through dynamic simulations. Similar to case2, the same heat exchanger is placed upstream of the HPDC-U system. After heat transfer, outside air is cooled and dehumidified by the DX cooling coil and then further dehumidified by the desiccant wheel. The dry air is mixed with the return air and delivered to the PTAC for temperature regulation. Fig. 3 shows the system configuration and air handling process in the psychrometric chart.

2.2 Building model and simulation setup

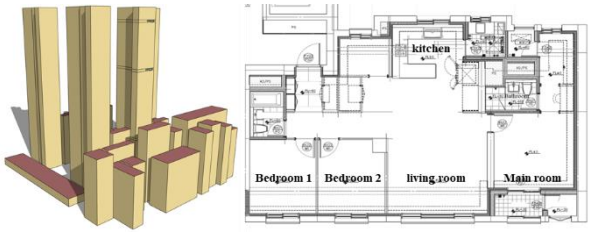

Fig. 4 – Building geometry and multi-zone floor plan.

Tab. 1 - Details of the target building.

Conditions	Detail setting
Simulation period	8/1 – 8/7
U-value (W/m^2·K)	wall: 0.211
	ceiling: 0.768
	floor: 0.768
	window: 0.834
Internal gain	people: 120 W/person
	light: 6.19 W/m^2
	household equipment: 160 W
	cooking: 15 W
Infiltration	maximum: 0.3 ACH
Internal carbon dioxide source	people: 3.82E-8 m^3/s·W
	cooking: 9.465E-5 m^3/s
Indoor T/RH	26 °C and 50 %
People schedule	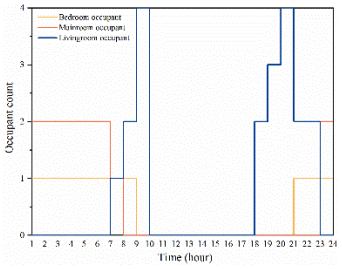

HPDC-U systems with a small size and simple structure can be potentially used in residential buildings with a low sensible and latent load. There is a tendency for residential buildings to develop into high-rise buildings, and the strengthening of airtightness in high-rise buildings makes it difficult to discharge indoor moisture. Therefore, we choose a three-bedroom apartment on the 69th floor of a high-rise building with high airtightness as the object of multi-zone analysis. The building geometry and room distribution are shown in the Fig. 4. Information about the building envelope and internal heat sources is summarized in Tab. 1. The carbon dioxide generation rate per unit of activity level is set at 3.82E-8 m^3/s·W according to the ASHRAE standard 62.1, and the carbon dioxide generation rate during cooking is taken as 9.465E-5 m^3/s and released for ten minutes with reference to the research results of Yujiao Zhao et al. [27]. Seoul (37° 33'N, 126°58'E) were selected as the outdoor conditions where has higher outdoor humidity in the summer than other cities with the same latitude, and the outdoor temperatures is below 30 °C most of the time which means that low outdoor temperatures are more conducive to the verification of the effect of condensing heat regeneration. We choose the week with the highest outdoor temperature and humidity as the simulation period (8/1-8/7), while the system energy use analysis is done for the entire summer (6/1-9/30).

3. System modelling and validation

3.1 Desiccant wheel modelling

$$\begin{bmatrix} T'_{ro} \\ w'_{ro} \end{bmatrix} = \begin{bmatrix} i_2 & i_3 & i_4 & i_5 & i_6 & i_7 & i_8 \\ j_2 & j_3 & j_4 & j_5 & j_6 & j_7 & j_8 \end{bmatrix} \begin{bmatrix} w_{ri} \\ T_{ri} \\ w_{ri}/T_{ri} \\ w_{pi} \\ T_{pi} \\ w_{pi}/T_{pi} \\ u \end{bmatrix} + \begin{bmatrix} i_1 \\ j_1 \end{bmatrix} \quad (1)$$

EnergyPlus mainly uses the dehumidification performance curve to establish the desiccant wheel model. Dehumidification performance curves are as shown in equation (1), reflecting the relationship between the inlet and outlet air state of both sides of the desiccant wheel. Where *w* is the air humidity ratio in kg/kg DA, T is the air temperature in °C, and *u* is the air flow rate in m/s. The subscript *pi*, *po*, *ri*, *ro* in following equations represents the inlet and outlet of the dehumidification side and regeneration side of the desiccant wheel. The curve coefficients *i* and *j* can be obtained by fitting measurement data or the results from other mathematical models that accurately reflect the performance of a balanced flow desiccant heat exchanger.

This regeneration side outlet air state is the state when the desiccant wheel is operated under full load condition. For part load operation, the actual regeneration side outlet air state could be modified by the part-load ratio (PLR) as shown from equation (2) to equation (4). ΔT_r and Δw_r are the

temperature difference and humidity difference of regeneration side under the full load condition, respectively.

$$\begin{bmatrix}\Delta T_r\\ \Delta w_r\end{bmatrix} = \begin{bmatrix}T'_{ro} - T_{ri}\\ w'_{ro} - w_{ri}\end{bmatrix} \quad (2)$$

$$PLR = \frac{w_{pi} - w_{setpoint}}{\Delta w_r} \quad (3)$$

$$\begin{bmatrix}T_{ro}\\ w_{ro}\end{bmatrix} = \begin{bmatrix}T_{ri} + \Delta T_r \times PLR\\ w_{ri} - \Delta w_r \times PLR\end{bmatrix} \quad (4)$$

Then, the sensible heat and latent heat change in the regeneration side of the desiccant wheel can be obtained by equation (5). Where $c_{p,r}$ and h_v are the specific heat of regeneration air and the latent heat of vaporization of water, respectively.

$$\begin{bmatrix}Q_{sensible,\ Reg}\\ Q_{latent,\ Reg}\end{bmatrix} = \begin{bmatrix}m_r c_{p,r}(T_{ro} - T_{ri})\\ m_r h_v(w_{ro} - w_{ri})\end{bmatrix} \quad (5)$$

In addition, the dehumidification side outlet air state can be accordingly calculated using the principle of mass and energy conservation as shown in equation (6), where $c_{p,p}$ is the specific heat of process air.

$$\begin{bmatrix}T_{po}\\ w_{po}\end{bmatrix} = \begin{matrix}T_{pi} - \frac{Q_{sensible,\ Reg}}{m_p c_{p,p}}\\ \left\lfloor W_{pi} - \frac{Q_{latent,\ Reg}}{m_p h_v}\right\rfloor\end{matrix} \quad (6)$$

3.2 Direct expansion coil modelling

DX cooling coil model in EnergyPlus is used since the heat pump operates only in the cooling mode. In EnergyPlus, the actual operational state of the DX cooling coil is determined by the total cooling capacity (TCC) modification curve (MC) and energy input rate (EIR) modification curve. Equation (7) and equation (8) depict the performance curves related to the inlet wet bulb temperature of the evaporator (T_{w_ei}), inlet dry bulb temperature (T_{ci}) of the condenser, and airflow rate (V).

$$\begin{bmatrix}MC_{TCC\_T}\\ MC_{EIR\_T}\end{bmatrix} = \begin{bmatrix}a_1\\ c_1\end{bmatrix} + \begin{bmatrix}a_2 a_3 a_4 a_5 a_6\\ c_2 c_3 c_4 c_5 c_6\end{bmatrix} \begin{matrix}T_{w\_ei}\\ T_{w\_ei}^2\\ T_{ci}\\ T_{ci}^2\\ \lfloor T_{w\_ei} T_{ci}\rfloor\end{matrix} \quad (7)$$

$$\begin{bmatrix}MC_{TCC\_F}\\ MC_{EIR\_F}\end{bmatrix} = \begin{bmatrix}b_1\\ d_1\end{bmatrix} + \begin{bmatrix}b_2 & b_3\\ d_2 & d_3\end{bmatrix}\begin{bmatrix}V\\ V^2\end{bmatrix} \quad (8)$$

The coefficients of the modification curve are the same as those used in the prior study [22].

3.3 Heat exchanger wheel modelling

Generally, heat-exchanger effectiveness for balanced flow is evaluated by equation (9).

$$\varepsilon = \frac{T_i - T_o}{T_i - T_e} \quad (9)$$

where T_i and T_o are the inlet and outlet air temperature of the supply flow side. T_e is the inlet air temperature of the secondary flow side.

As the equation (10) and equation (11), the model in this study determines the actual sensible (latent) heat transfer effectiveness by linear interpolation or extrapolation of the 100% flow and 75% flow sensible (latent) heat transfer effectiveness values, ε_{s_100} (ε_{l_100})and ε_{s_75} (ε_{l_75}). These values used in this study are obtained from the Air-Conditioning and Refrigeration Institute's Certified Product Directory for Air-to-Air Energy Recovery Ventilation Equipment and listed in Tab. 3. HX_{fr} is the ratio of the average operating volumetric air flow rate [(supply flow + exhaust flow)/2] to the norminal supply air flow rate.

$$\varepsilon_{op\_s} = \varepsilon_{s\_75} + (\varepsilon_{s\_100} - \varepsilon_{s\_75})\left(\frac{HX_{fr} - 0.75}{1 - 0.75}\right) \quad (10)$$

$$\varepsilon_{op\_l} = \varepsilon_{l\_75} + (\varepsilon_{l\_100} - \varepsilon_{l\_75})\left(\frac{HX_{fr} - 0.75}{1 - 0.75}\right) \quad (11)$$

Tab. 3- Effectiveness values of heat recovery wheel.

	Heating	Cooling
ε_{s_75}	0.75	0.75
ε_{s_100}	0.72	0.72
ε_{l_75}	0.73	0.73
ε_{l_100}	0.7	0.63

According to the equation (12) to (14), the supply air conditions (T_{1o} and w_{1o}) leaving the heat exchanger are determined using the operating effectiveness calculated above, the ratio of the air stream with the minimum heat capacity rate, $\dot{m}c_{p,min}$, to the supply air stream heat capacity rate, $\dot{m}c_{p,1}$, and the difference in temperature or humidity ratio between the supply and exhaust inlet air with subcript 1i and 2i, respectively.

$$\dot{m}c_{p,min} = \min(\dot{m}c_{p,1}, \dot{m}c_{p,2}) \quad (12)$$

$$T_{1o} = T_{1i} + \varepsilon_{op\_s} \cdot \left(\frac{\dot{m}c_{p,min}}{\dot{m}c_{p,1}}\right) \cdot (T_{2i} - T_{1i}) \quad (13)$$

$$w_{1o} = w_{1i} + \varepsilon_{op\_l} \cdot \left(\frac{\dot{m}c_{p,min}}{\dot{m}c_{p,1}}\right) \cdot (w_{2i} - w_{1i}) \quad (14)$$

4. Simulation results

4.1 Indoor humidity and IAQ in case 1

Fig. 5 shows the variation of indoor humidity during the PTAC operation and the shaded areas in different colours represents the people schedule of each room. Since the two bedrooms have the same orientation, size and number of people, the humidity variation in the bedroom remains almost the same. Except for a brief increase in humidity caused by an increase in the number of people, the humidity in

the room can be continuously reduced due to the wet coil state operated DX cooling coil in PTACs. For a bedroom with only one person, indoor humidity can be reduced to 50 % in a short time. For the livingroom with a brief high people density and the mainroom with two persons, the indoor humidity is unable to be dropped below 50 % within the occupancy time. In addition, since the bedroom has a relatively small area and good airtightness, the indoor CO_2 concentration tends to increase and can reach up to 3686 ppm. The CO_2 concentration exceeds the recommended level all of the occupancy period. The CO_2 concentration in other large rooms can reach up to 2158 ppm and 3246 ppm respectively. Moreover, the time that indoor CO_2 concentration exceeded the recommended level accounts for 94 % and 74 % of the total occupancy time for livingroom and mainroom.

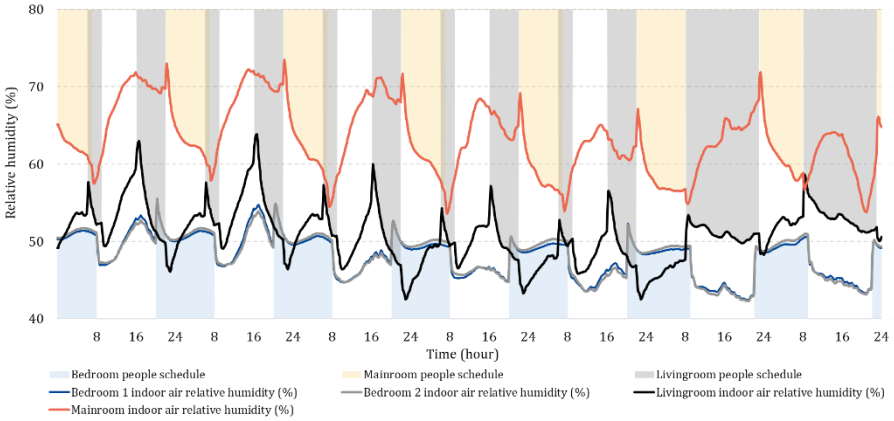

Fig. 5 – Variation of the indoor humidity during PTACs operation.

4.2 The effect of DCV on indoor humidity and IAQ

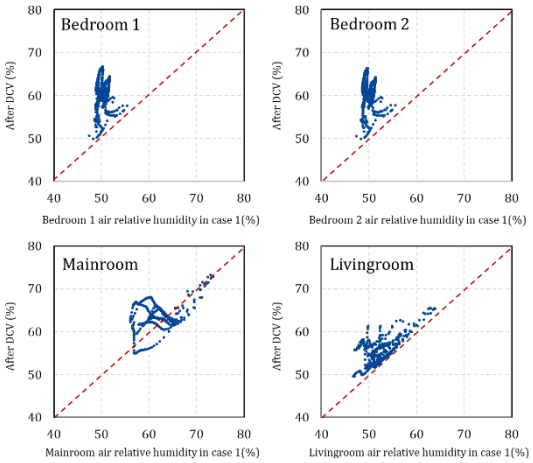

Fig. 6 –Indoor relative humidity after the introduction of outdoor fresh air during occupancy period.

After the introduction of outdoor fresh air, there is a significant increase in indoor humidity in each room compared to case1 during the occupancy period as shown in Fig. 6. There is a situation that the indoor humidity in the mainroom is lower than case1, which is mainly due to the fact that the outdoor humidity ratio is lower than the indoor humidity ratio during the night ventilation, therefore it achieves a certain free-dehumidification effect.

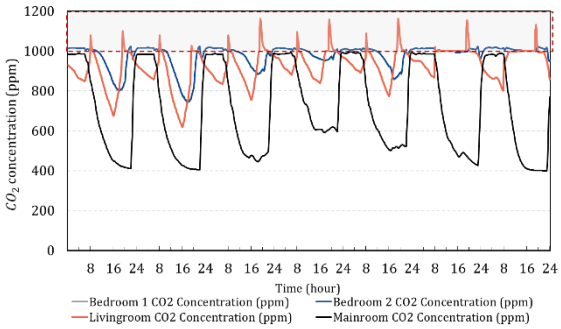

Fig. 7 – Changes in indoor CO_2concentration after the introduction of outdoor fresh air.

Fig. 7 indicates that the DCV method can effectively control the CO_2 concentration in each room. For the livingroom, the CO_2 generated during cooking for a short period of time can cause the CO_2 concentration to spike, however, the time that the CO_2 concentration exceeds the recommended level only accounts for 8 % of the total occupancy time. Therefore, we propose the multi-zone applicable HPDC-U system that can maintain the indoor humidity environment while controlling IAQ by DCV method.

4.3 Indoor environment control effect and energy use of the HPDC-U system

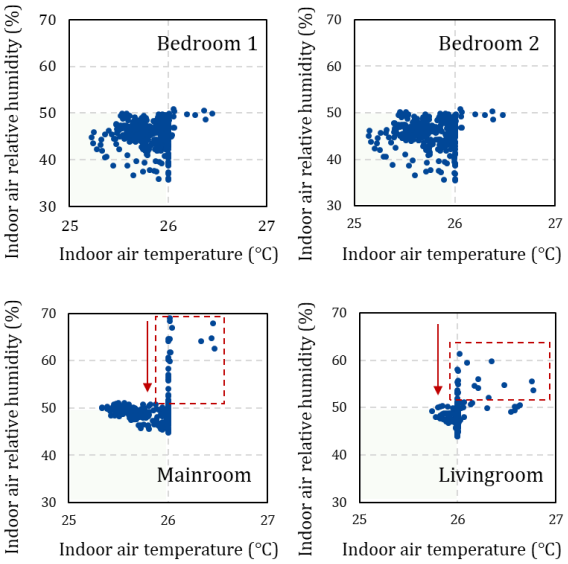

Fig. 8 – Indoor temperature and humidity state during the occupancy period.

Fig. 8 shows the state of indoor temperature and humidity during the occupancy period in each room. For bedrooms with small changes in indoor sensible and latent loads, the indoor temperature and humidity control is relatively stable, with only a brief temperature rise of about 0.5 °C when people enter. Limited by the DCV determined outdoor air volume, the HPDC-U system has insufficient instantaneous dehumidification capacity for multi-zone applications, allowing the indoor humidity in the mainroom and livingroom to decrease from high humidity to 50 % level over a period of time. The descent process corresponds to the data in the red box line in Fig. 8. The indoor temperature in each room is sometimes lower than the indoor design temperature. Under low indoor sensible and latent load conditions, after the pre-cooling and pre-dehumidification process in HPDC-U systems, the air humidity meets the demand of indoor latent load. Therefore, the desiccant wheel does not need to be started. The PTAC in each room also does not require re-cooling of the air, and the approximately 22 °C mixed air is directly supply into the room which leads to the low indoor temperature.

From the Fig. 9, it can be seen that the maximum monthly energy use of both case3 and case2 occurs in August when the outdoor temperature and humidity are high. The monthly energy use of case3 is slightly lower than that of case2 in June and September, while it is higher than that of case2 in July and August as the humidity increases. The total energy use in summer of case2 and case3 is 605 kWh and 606 kWh, respectively, which means that the setup of the HPDC-U system does not lead to an increase in the total system energy use.

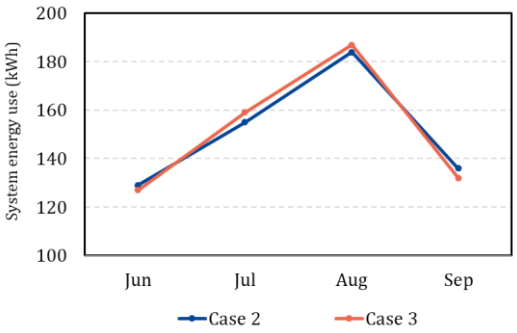

Fig. 9 – Monthly energy use comparison between case2 and case3.

Fig. 10 indicates the energy use comparison of each energy consuming component in the two systems. With the HPDC-U system, the energy use of PTACs in each room is able to be reduced significantly due to the fact that the desiccant wheel can reduce the latent heat treated by the PTAC and increase the sensible heat ratio of PTACs (SHR) and the dry coil state operation time. Energy use of the PTAC in the livingroom with higher latent load can be reduced by 40 %. However, the total energy use of the HPDC-U system as an OAU is much greater than that of the heat recovery wheel assisted OAU, therefore, the total energy use of the OAU and zone level PTACs in both cases is almost equal. The ability of case3 to maintain the indoor thermal environment and IAQ without increasing energy use proves that it is a viable alternative system for existing systems in multi-zone.

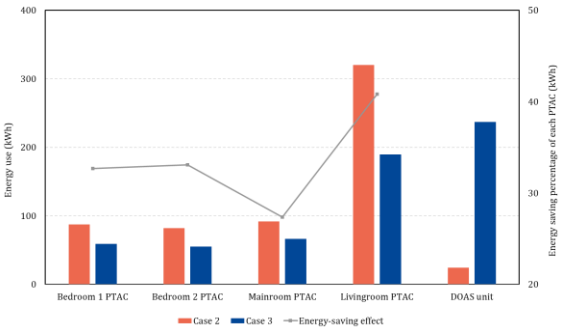

Fig. 10 – Energy use comparison of OAU and PTACs for case2 and case3.

Acknowledgement

This work was supported by the National Research Foundation of Korea grant (2021R1A2C1014415) funded by the Ministry of Science and ICT (South Korea) (MIST). We thank Humaster Co. for technical data support in desiccant wheel modelling.

References

[1] Arundel A V., Sterling EM, Biggin JH, Sterling TD. Indirect health effects of relative humidity in indoor environments. Environ Health Perspect. 1986; 65(3):351–61.

[2] Li Z, Chen W, Deng S, Lin Z. The characteristics of space cooling load and indoor humidity control

for residences in the subtropics. Build Environ. 2006;41(9):1137–47.
[3] Katili AR, Boukhanouf R, Wilson R. Space Cooling in Buildings in Hot and Humid Climates—A Review of the Effect of Humidity on the Applicability of Existing Cooling Techniques. Proc 14th Int Conf Sustain Energy Technol. 2015;(August):25–7.
[4] Bakker A, Siegel JA, Mendell MJ, Peccia J. Building and environmental factors that influence bacterial and fungal loading on air conditioning cooling coils. Indoor Air. 2018;28(5):689–96.
[5] Fong KF, Lee CK, Chow TT, Fong AML. Investigation on solar hybrid desiccant cooling system for commercial premises with high latent cooling load in subtropical Hong Kong. Appl Therm Eng. 2011;31(16):3393–401.
[6] Jani DB, Mishra M, Sahoo PK. Performance studies of hybrid solid desiccant-vapor compression air-conditioning system for hot and humid climates. Energy Build. 2015;102:284–92.
[7] Hwang WB, Choi S, Lee DY. In-depth analysis of the performance of hybrid desiccant cooling system incorporated with an electric heat pump. Energy. 2017;118:324–32.
[8] Kashif Shahzad M, Ali M, Ahmed Sheikh N, Qadar Chaudhary G, Shahid Khalil M, Rashid TU. Experimental evaluation of a solid desiccant system integrated with cross flow Maisotsenko cycle evaporative cooler. Appl Therm Eng. 2018;128:1476–87.
[9] Elgendy E, Mostafa A, Fatouh M. Performance enhancement of a desiccant evaporative cooling system using direct/indirect evaporative cooler. Int J Refrig. 2015;51:77–87.
[10] Jani DB, Mishra M, Sahoo PK. A critical review on solid desiccant-based hybrid cooling systems. Int J Air-Conditioning Refrig. 2017;25(3):1–10.
[11] Shamim JA, Hsu WL, Paul S, Yu L, Daiguji H. A review of solid desiccant dehumidifiers: Current status and near-term development goals in the context of net zero energy buildings. Renew Sustain Energy Rev. 2021;137(September 2020):110456.
[12] Yao Y, Dai L, Jiang F. Photo-crosslinked nanofibrous membranes as advanced low-temperature regenerative desiccant. Polym Test. 2019;78.
[13] Habib MF, Ali M, Sheikh NA, Badar AW, Mehmood S. Building thermal load management through integration of solar assisted absorption and desiccant air conditioning systems: A model-based simulation-optimization approach. J Build Eng. 2020;30(February):101279.
[14] Kashif A, Ali M, Sheikh NA, Vukovic V, Shehryar M. Experimental analysis of a solar assisted desiccant-based space heating and humidification system for cold and dry climates. Appl Therm Eng. 2020;175(April).
[15] Li H, Dai YJ, Köhler M, Wang RZ. Simulation and parameter analysis of a two-stage desiccant cooing/heating system driven by solar air collectors. Energy Convers Manag. 2013;67:309–17.
[16] Sheng Y, Zhang Y, Deng N, Fang L, Nie J, Ma L. Experimental analysis on performance of high temperature heat pump and desiccant wheel system. Energy Build. 2013;66:505–13.
[17] Jia CX, Dai YJ, Wu JY, Wang RZ. Analysis on a hybrid desiccant air-conditioning system. Appl Therm Eng. 2006;26(17–18):2393–400.
[18] Nie J, Fang L, Zhang G, Sheng Y, Kong X, Zhang Y, et al. Theoretical study on volatile organic compound removal and energy performance of a novel heat pump assisted solid desiccant cooling system. Build Environ. 2015;85:233–42.
[19] Nie J, Li Z, Hu W, Fang L, Zhang Q. Theoretical modelling and experimental study of air thermal conditioning process of a heat pump assisted solid desiccant cooling system. Energy Build. 2017;153:31–40.
[20] Ge F, Wang C. Exergy analysis of dehumidification systems: A comparison between the condensing dehumidification and the desiccant wheel dehumidification. Energy Convers Manag. 2020;224(September):113343.
[21] Belguith S, Slama R Ben, Chaouachi B, Meddeb Z. Performance analysis of hybrid solid desiccant-vapor compression air conditioning system: Application and comparative study. 11th Int Renew Energy Congr IREC 2020. 2020;(Irec).
[22] Liu S, Jeong CH, Yeo MS. Effect of evaporator position on heat pump assisted solid desiccant cooling systems. Energies. 2020;13(22):1–21.
[23] Afroz Z, Higgins G, Shafiullah GM, Urmee T. Evaluation of real-life demand-controlled ventilation from the perception of indoor air quality with probable implications. Energy Build. 2020;219.
[24] Schibuola L, Scarpa M, Tambani C. CO2 based ventilation control in energy retrofit: An experimental assessment. Energy. 2018;143:606–14.
[25] Merema B, Delwati M, Sourbron M, Breesch H. Demand controlled ventilation (DCV) in school and office buildings: Lessons learnt from case studies. Energy Build. 2018;172:349–60.
[26] Sun Z, Wang S, Ma Z. In-situ implementation and validation of a CO2-based adaptive demand-controlled ventilation strategy in a multi-zone office building. Build Environ. 2011;46(1):124–33.
[27] Zhao Y, Li A, Gao R, Tao P, Shen J. Measurement of temperature, relative humidity and concentrations of CO, CO2 and TVOC during cooking typical Chinese dishes. Energy Build. 2014;69:544–61.